RÅC INTERNATIONAL SUMMER SCHOOL 2025

Advanced Materials Design at X-ray and Neutron Facilities

AI in Spectroscopy

LATVIJAS UNIVERSITĀTES
CIETVIELU FIZIKAS INSTITŪTS
INSTITUTE OF SOLID STATE PHYSICS
UNIVERSITY OF LATVIA

Dr.phys. Alexei Kuzmin

Head of the EXAFS Spectroscopy Laboratory

E-mail: a.kuzmin@cfi.lu.lv

https://www.dragon.lv/exafs

EXAFS Lab

Talk Outline

- Introduction
- General machine learning concepts
- AI methods in X-ray absorption spectroscopy
- Examples of forward and inverse problem solving
- Conclusions

Introduction

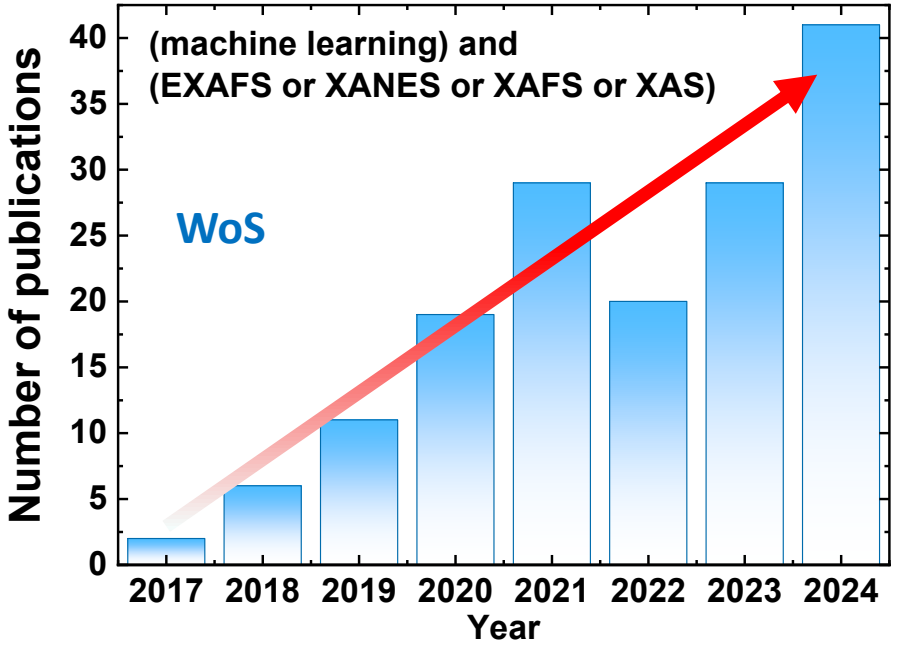

Experimental: ROI selection

research papers

JOURNAL OF SYNCHROTRON RADIATION
ISSN 1600-5775

Direct tomography imaging for inelastic X-ray scattering experiments at high pressure

Ch. J. Sahle,[a]* A. D. Rosa,[a] M. Rossi,[a] V. Cerantola,[a] G. Spiekermann,[b] S. Petitgirard,[c] J. Jacobs,[a] S. Huotari,[d] M. Moretti Sala[a] and A. Mirone[a]

[a]European Synchrotron Radiation Facility, 71 Avenue des Martyrs, 38000 Grenoble, France, [b]Institute of Earth and Environmental Science, Universität Potsdam, Potsdam, Germany, [c]Bayerisches Geoinstitut, University of Bayreuth, Bayreuth, Germany, and [d]Department of Physics, POB 64, FI-00014, University of Helsinki, Helsinki, Finland. *Correspondence e-mail: christoph.sahle@esrf.fr

Received 13 September 2016
Accepted 24 October 2016

J. Synchrotron Rad. 24, 269–275 (2017).

Data interpretation

THE JOURNAL OF PHYSICAL CHEMISTRY Letters
Letter
Cite This: J. Phys. Chem. Lett. 2017, 8, 5091-5098
pubs.acs.org/JPCL

Supervised Machine-Learning-Based Determination of Three-Dimensional Structure of Metallic Nanoparticles

Janis Timoshenko,*[,†] Deyu Lu,[‡] Yuewei Lin,[§] and Anatoly I. Frenkel*[,†,∥]

[†]Department of Material Science and Chemical Engineering, Stony Brook University, Stony Brook, New York 11794, United States
[‡]Center for Functional Nanomaterials, Brookhaven National Laboratory, Upton, New York 11973, United States
[§]Computational Science Initiative, Brookhaven National Laboratory, Upton, New York 11973, United States
[∥]Division of Chemistry, Brookhaven National Laboratory, Upton, New York 11973, United States

J. Phys. Chem. Lett. 8, 5091–5098 (2017).

How can Machine Learning Methods be used: Forward vs Inverse Problem

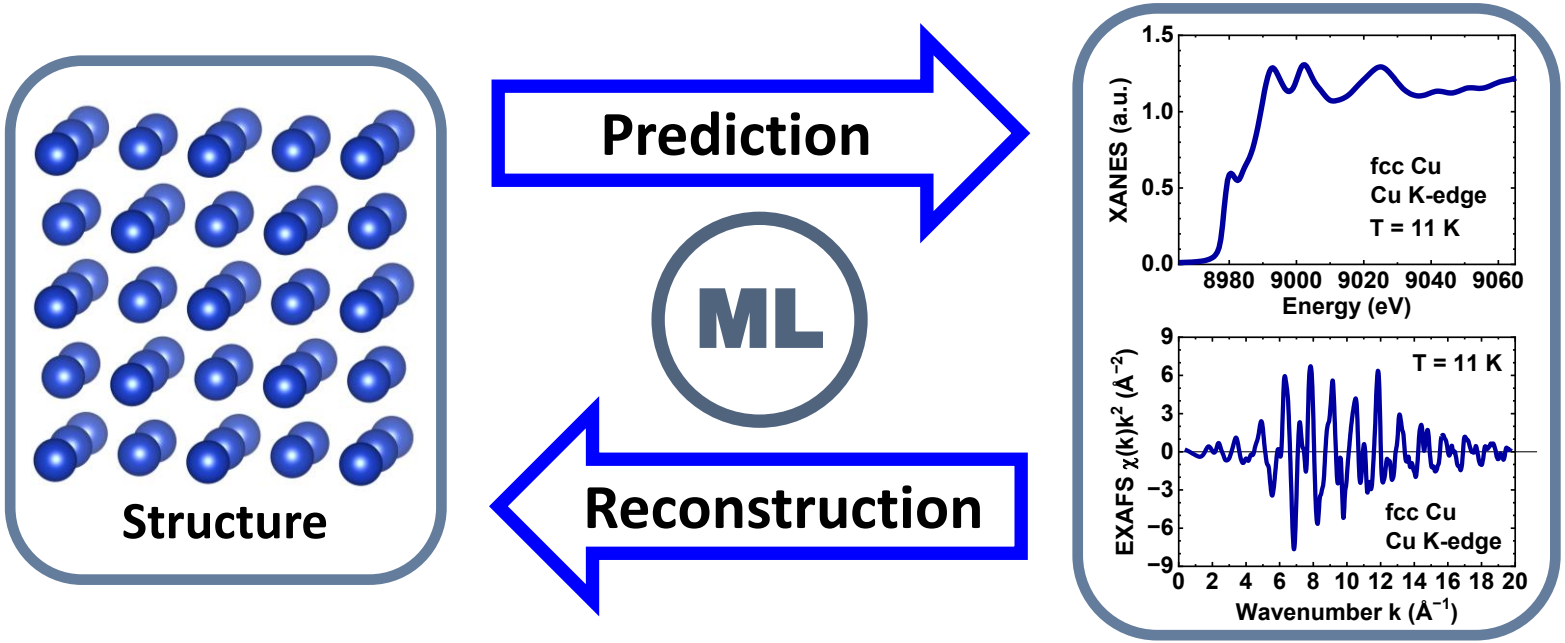

Basics of X-ray Absorption Spectroscopy (XAS)

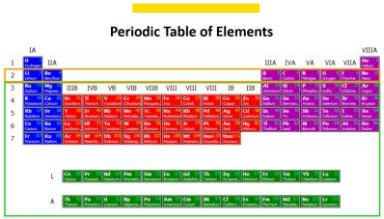

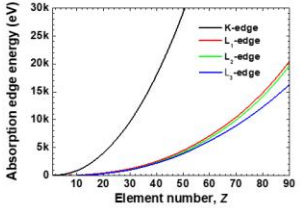

Fermi's Golden Rule:

$$\mu(E) \propto \sum_f \left|\langle f|\hat{H}|i\rangle\right|^2 \delta(E_f - E_i - \hbar\omega)$$

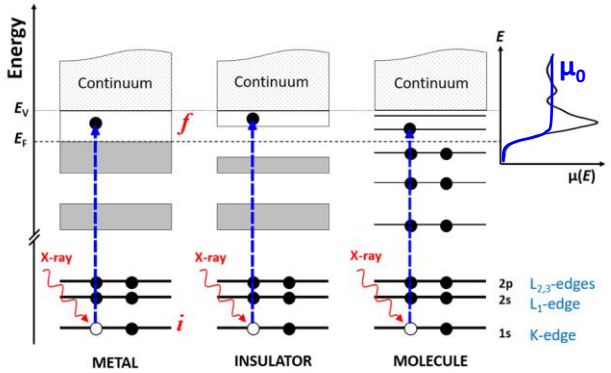

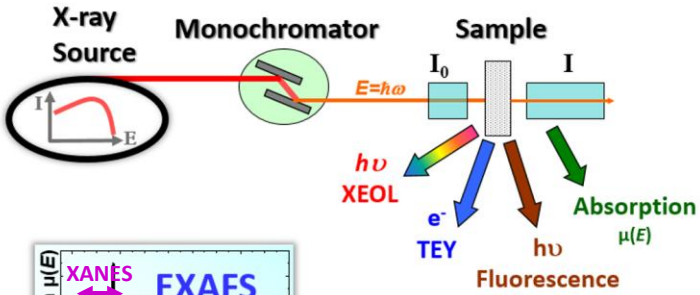

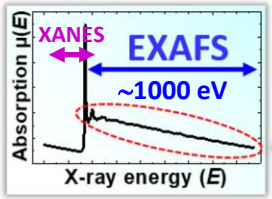

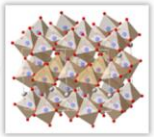

$$\mu(E) = \frac{1}{x}\ln\left(\frac{I_0(E)}{I(E)}\right)$$

$$\mu(E) \propto \frac{I_{\text{fluo}}(E)}{I_0(E)}$$

$$\mu(E) \propto \frac{I_{\text{TEY}}(E)}{I_0(E)}$$

$$\mu(E) \propto \frac{I_{\text{XEOL}}(E)}{I_0(E)}$$

Short range order **< 6-10 Å**

Characteristic time of X-ray absorption process:

$t_{ab} \sim 10^{-15}$-10^{-16} s

Characteristic time of thermal vibrations:

$t_{th} \sim 10^{-13}$-10^{-14} s

- Atoms are frozen during X-ray absorption
- Static & thermal disorder contribute similarly

The Effect of Thermal Disorder on EXAFS Amplitude

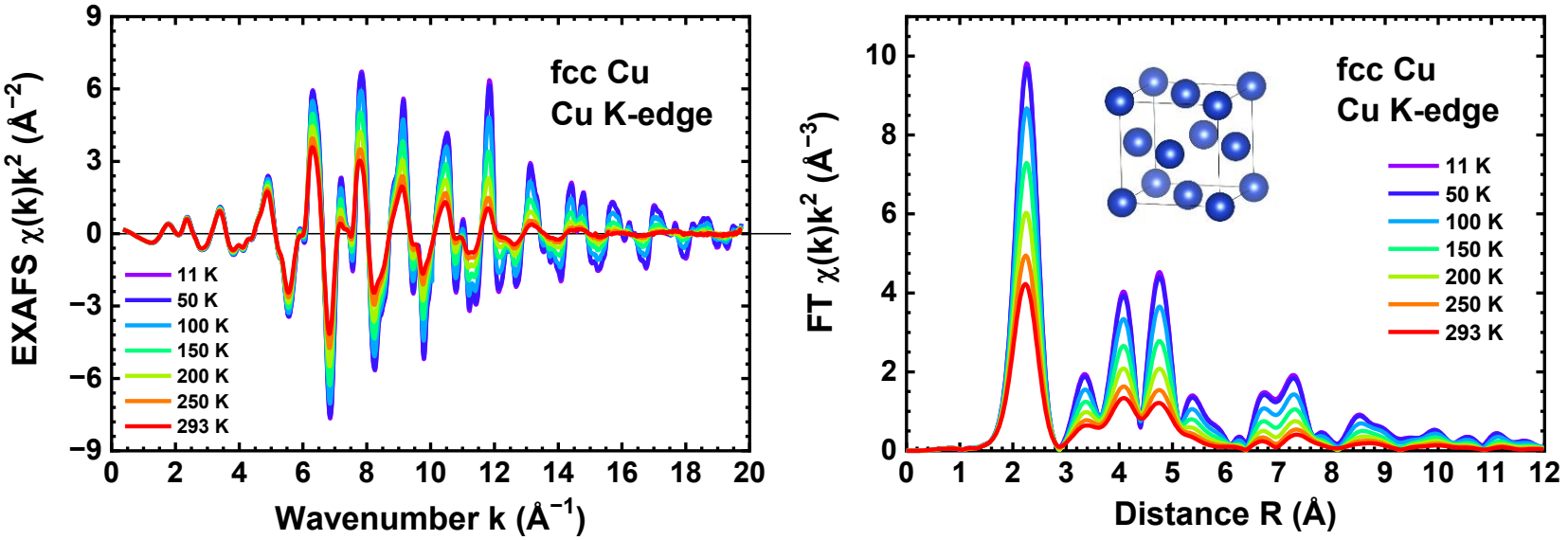

A. Kuzmin, V. Dimitrijevs, I. Pudza, A. Kalinko, Phys. Status Solidi A (2024) 2400623.

The Effect of Thermal Disorder on Interatomic Distances: EXAFS vs Diffraction

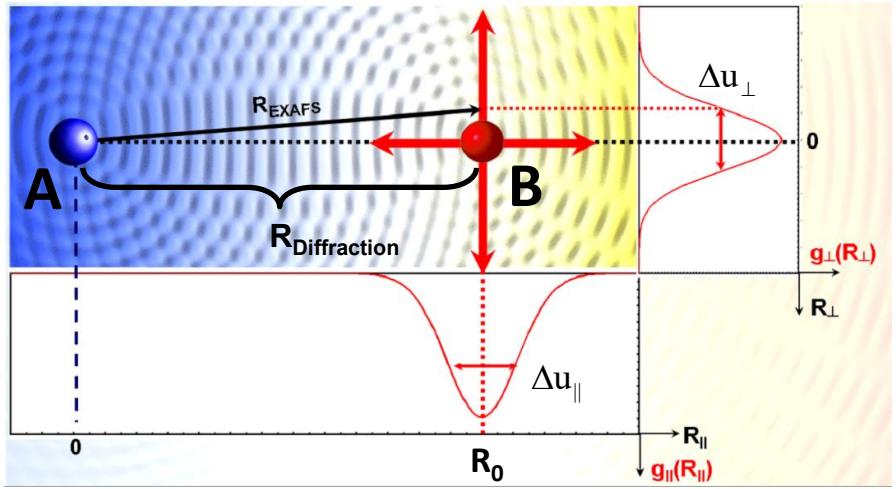

R_0 – equilibrium distance

$$R_{Diffraction} = |\langle \vec{r}_A \rangle - \langle \vec{r}_B \rangle|$$

$$R_{EXAFS} = \langle |\vec{r}_A - \vec{r}_B| \rangle$$

In harmonic approximation

$$R_{EXAFS} = R_{Diffraction} + \frac{\langle \Delta u_{\perp}^2 \rangle}{2R_{Diffraction}}$$

P. Fornasini, J. Phys.: Condens. Matter 13 (2001) 7859-7872.

Extended X-ray Absorption Fine Structure (EXAFS)

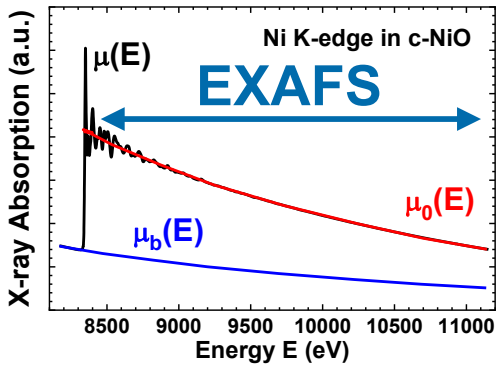

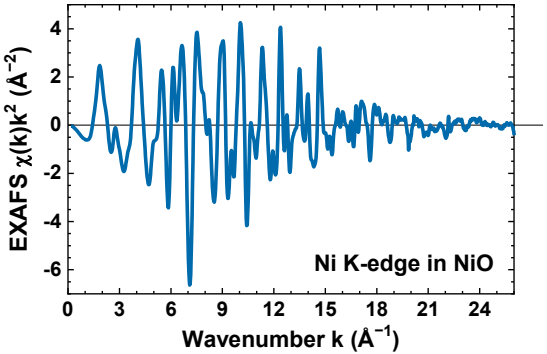

EXAFS spectrum:

$$\chi(k) = \frac{\mu(E) - \mu_b(E) - \mu_0(E)}{\mu_0(E)}$$

$$k = \sqrt{(2m_e/\hbar^2)(E - E_0)}$$

Multiple-scattering (MS) processes

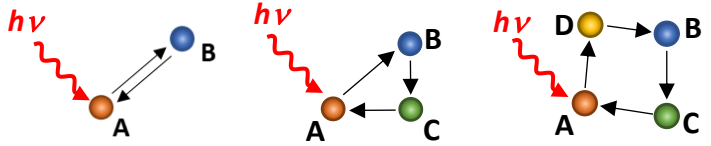

MS expansion of EXAFS in the presence of disorder:

$$\begin{aligned}
\chi(k) \;=\; & \int 4\pi R^2 \rho_0 g_2(R)(\chi_2^{oio}(k) + \chi_4^{oioio}(k) + \ldots)\mathrm{d}R \\
& + \iiint 8\pi^2 R_1^2 R_2^2 \sin(\theta)\rho_0^2 g_3(R_1, R_2, \theta) \\
& \times(2\chi_3^{oijo}(k) + 2\chi_4^{oiojo}(k) + \chi_4^{oijio}(k) + \chi_4^{ojijo}(k) + \ldots)\mathrm{d}R_1\mathrm{d}R_2\mathrm{d}\theta \\
& + \iiiint\!\!\int 8\pi^2 R_1^2 R_2^2 R_3^2 \sin(\theta)\rho_0^3 g_4(R_1, R_2, \theta, R_3, \Omega) \\
& \times(2\chi_4^{oijko}(k) + 2\chi_4^{oikjo}(k) + 2\chi_4^{ojiko}(k) + \ldots)\mathrm{d}R_1\mathrm{d}R_2\mathrm{d}\theta\mathrm{d}R_3\mathrm{d}\Omega \\
& + \ldots
\end{aligned}$$

g_n - n-atom distribution function

A. Filipponi, A. Di Cicco, C. R. Natoli, Phys. Rev. B 52 (1995) 15122-15134.

A Schematic of AI-ML-DL Context

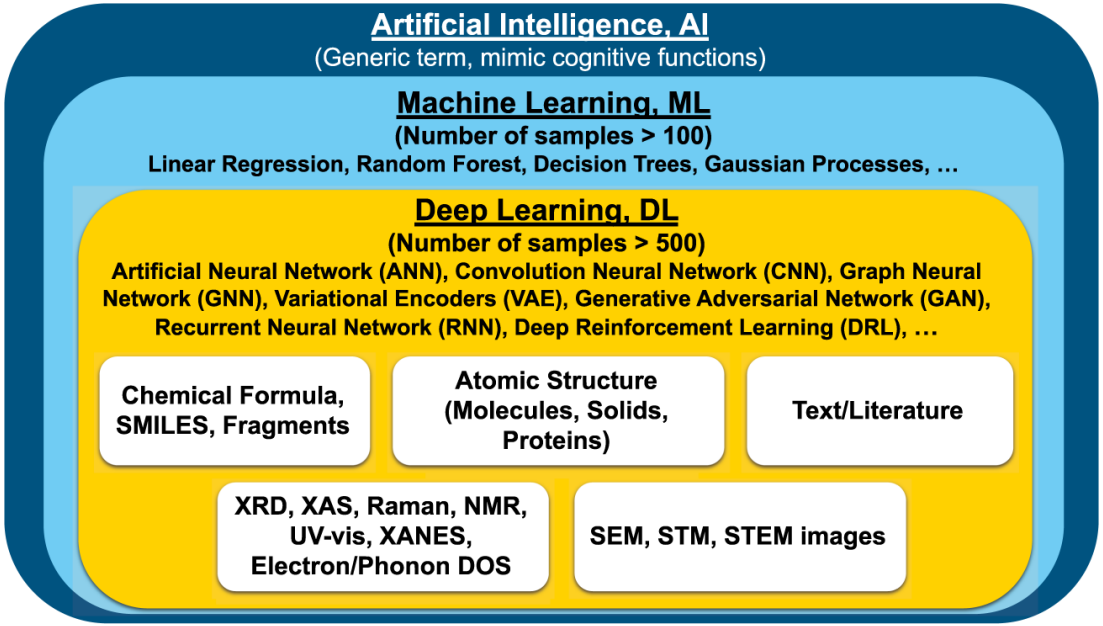

AI mimics intelligence, for example, by optimizing actions to achieve specific objectives.

ML is a subset of AI, providing the ability to learn without explicitly being programmed for a given dataset.

DL methods are based on **artificial neural networks** (ANNs) and allied techniques.

K. Choudhary, B. DeCost, C. Chen et al., Recent advances and applications of deep learning methods in materials science, npj Comput Mater 8 (2022) 59.

A Perceptron or a Single Artificial Neuron

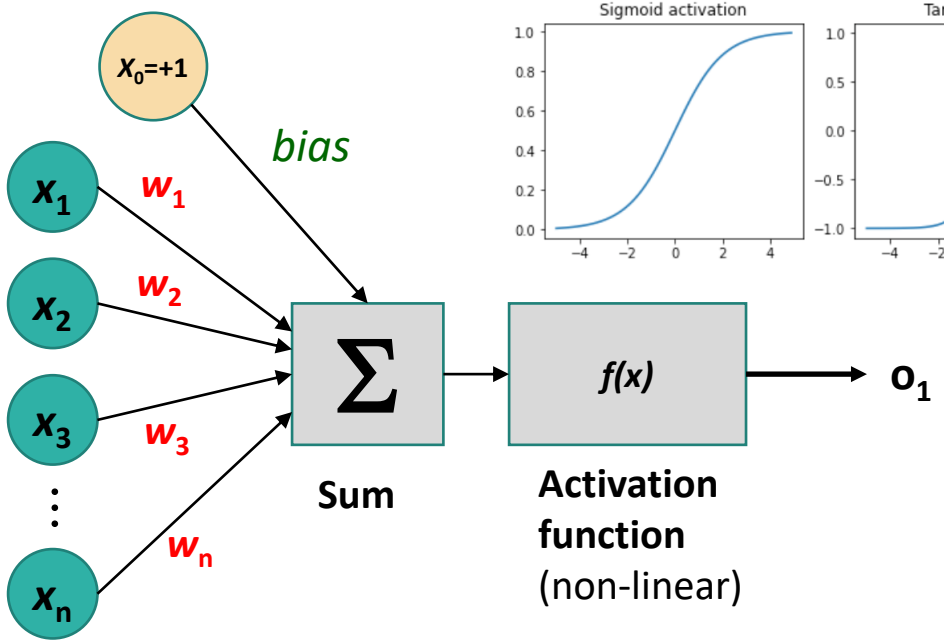

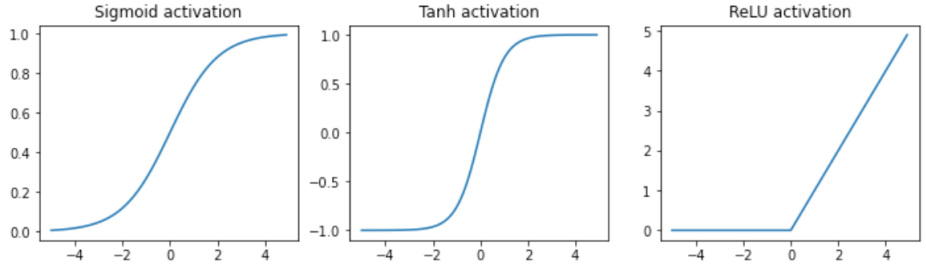

$$f(x) = f\left(bias + \sum_{i=1}^{n}(x_i w_i)\right)$$

When the activation function is non-linear, then a two-layer neural network can be proven to be a universal function approximator, i.e., it can approximate any continuous function to any desired degree of accuracy.

Artificial Neural Network (ANN)

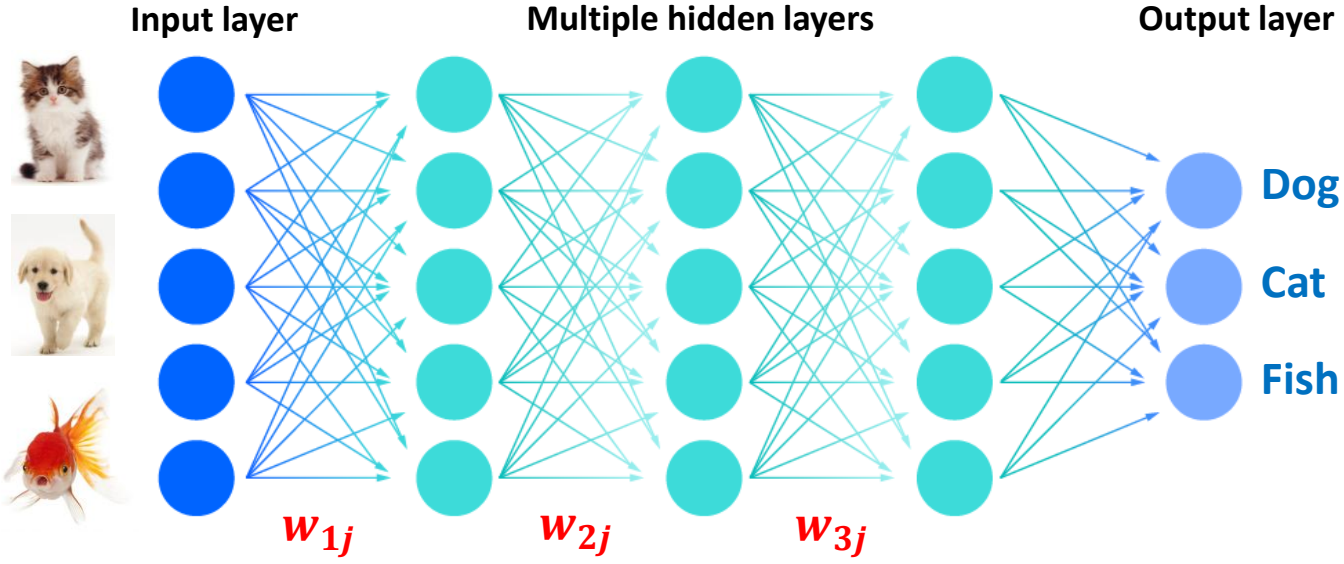

Big Dataset(s) → **Training**: $w_{ij} - ?$

Software for ANN training:

PyTorch

TensorFlow

mxnet

WOLFRAM MATHEMATICA

A Workflow for Structure Determination using X-ray Absorption Spectroscopy

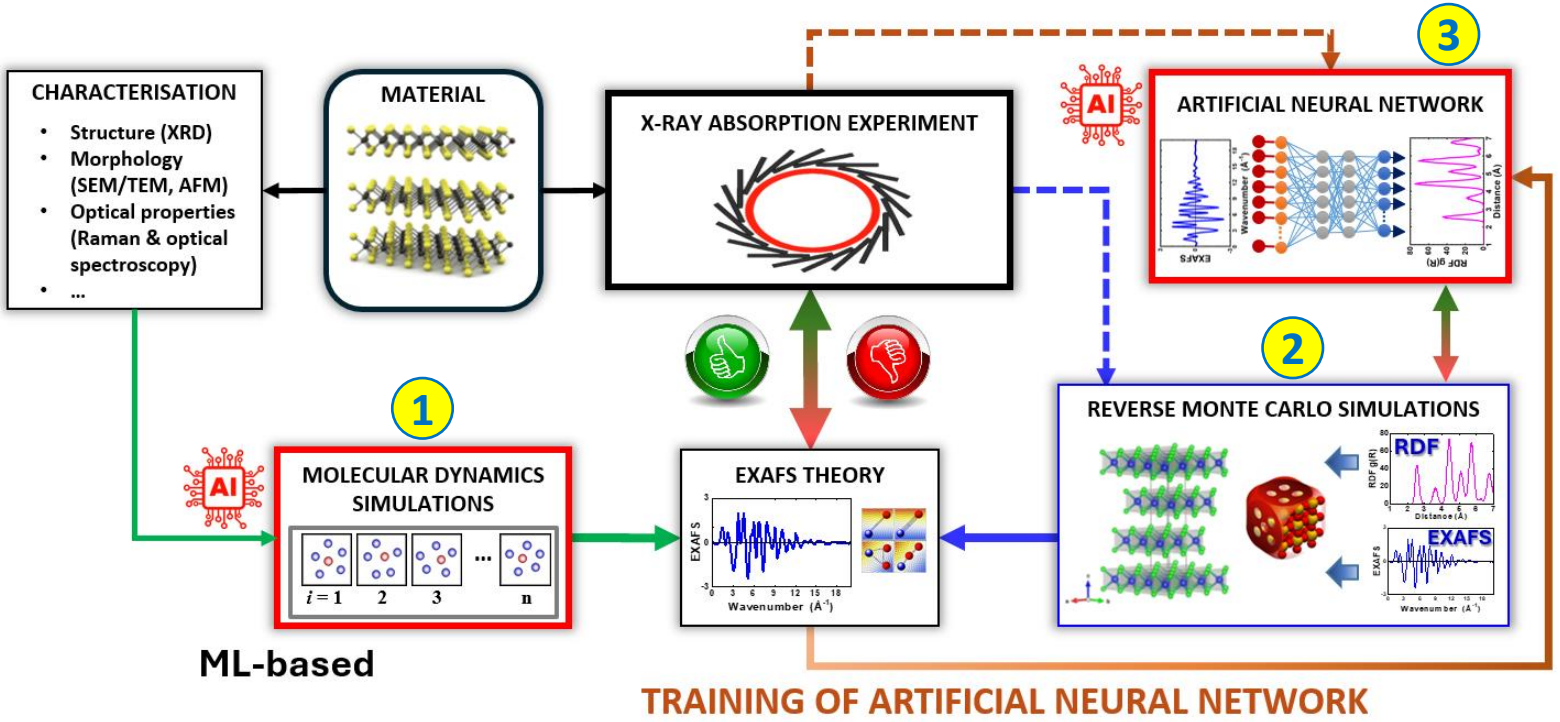

Molecular Dynamics Simulations of EXAFS Spectra (MD-EXAFS): History

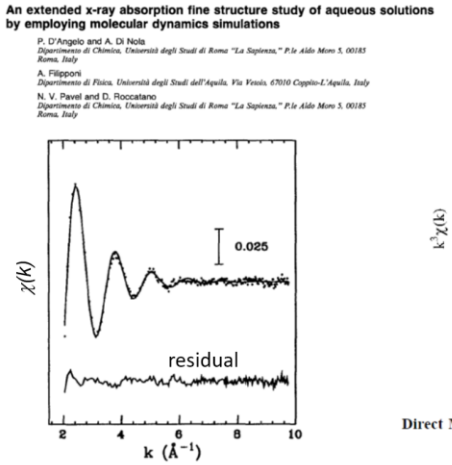

Br K-edge in 0.15M RbBr aqueous solution

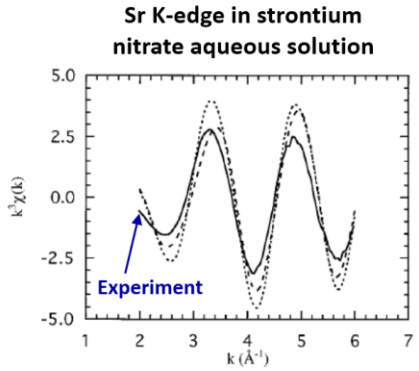

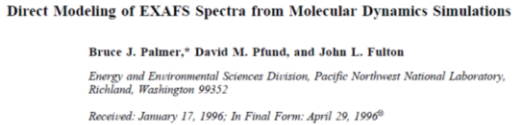

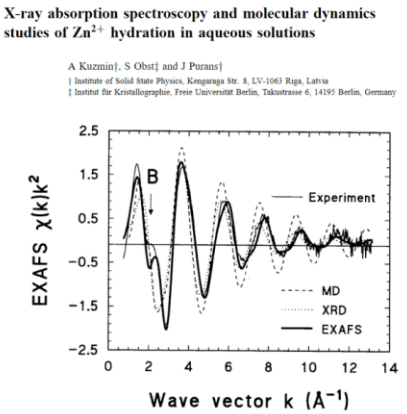

Zn K-edge in the 0.125M aqueous solution of $ZnSO_4$

[1] P. D'Angelo, A.D. Nola, A. Filipponi, N.V. Pavel, D. Roccatano, J. Chem. Phys. 100 (1994) 985-994.
[2] P. D'Angelo, A.D. Nola, M. Mangoni, N.V. Pavel, J. Chem. Phys. 104 (1996) 1779-1790.
[3] B.J. Palmer, D.M. Pfund, J.L. Fulton, J. Phys. Chem. 100 (1996) 13393.
[4] A. Kuzmin, S. Obst, J. Purans, J. Phys.: Condensed Matter 9 (1997) 10069-10078.

aqueous solutions

Molecular Dynamics Simulations of EXAFS Spectra (MD-EXAFS)

Code is available at https://www.dragon.lv/edaca/

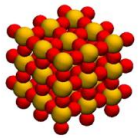

Initial structural model (supercell)

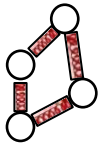

Interaction Model

$$U = \sum_i U^{(1)}(\vec{r}_i) + \sum_{i,j} U^{(2)}(\vec{r}_i, \vec{r}_j) + \cdots$$

Molecular Dynamics Ensemble

NVT, NpT, NVE, …

Molecular Dynamics Simulation

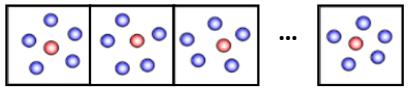

Calculation of configuration averaged EXAFS

$$\chi^{l}_{\mathrm{ca}}(k) = \left\langle \chi^{l}_{i}(k) \right\rangle$$

⇔ **Experiment**

Analysis of atomic configurations

RDF & BADF

New trend: Machine Learning Interatomic Potentials (MLIPs)

[1] A. V. Shapeev, D. Bocharov, A. Kuzmin, Comput. Mater. Sci. 210 (2022) 111028.
[2] P. Žguns, I. Pudza, A. Kuzmin, J. Chem. Theory Comput. 21 (2025) 8142–8150.

Reverse Monte Carlo (RMC) Approach to EXAFS: History

Reverse Monte Carlo simulation for the analysis of EXAFS data

S J Gurman† and R L McGreevy‡
† Department of Physics, University of Leicester, Leicester LE1 7RH, UK
‡ Clarendon Laboratory, Parks Road, Oxford OX1 3PU, UK

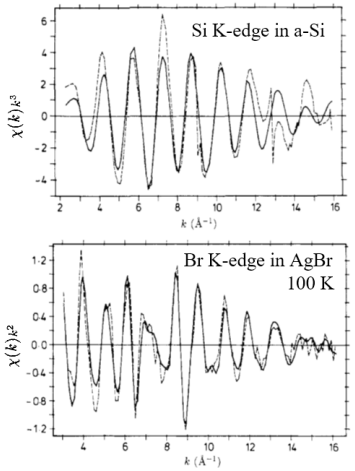

High temperature EXAFS experiments on liquid KPb alloys analysed with the reverse Monte Carlo method

W. Bras [a,b,*], R. Xu [c], J.D. Wicks[d,1], F. van der Horst [c], M. Oversluizen [a,b], R.L. McGreevy [e], W. van der Lugt [c]
[a] Netherlands Organisation for Scientific Research (NWO), The Netherlands
[b] SERC Daresbury Laboratory, Warrington WA4 4AD, UK
[c] Laboratory for Solid State Physics, Groningen University, Nyenborgh 18, 9747 AG Groningen, The Netherlands
[d] Clarendon Laboratory, Parks Road, Oxford, OX1 3PU, UK
[e] Studsvik Neutron Research Laboratory, Uppsala University, S-61182 Nyköping, Sweden

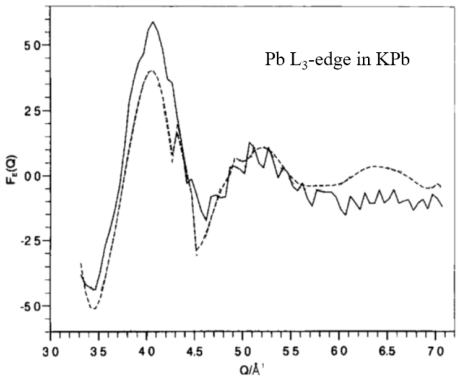

Fig. 4. EXAFS data, $F_E(Q)$, for molten KPb (solid line) compared to the RMC fit with 100% Zintl ions maintained (dotted line)

Modelling the Structure and Ionic Conduction of $(AgI)_x(AgPO_3)_{1-x}$ Glasses

J. D. Wicks,[1] L. Börjesson,[2] G. Bushnell-Wye,[3] W. S. Howells[4] and R. L. McGreevy[5]
[1] Department of Physics and Astronomy, University College London, Gower Street, London WC1E 6BT, U.K.
[2] Department of Physics, Royal Institute of Technology, S-100 44 Stockholm, Sweden
[3] SRS Daresbury Laboratory, Warrington, Cheshire WA4 4AD, U.K.
[4] ISIS Science Division, Rutherford Appleton Laboratory, Chilton, Didcot, Oxon OX11 0QX, U.K.
[5] Studsvik Neutron Research Laboratory, S-611 82 Nyköping, Sweden

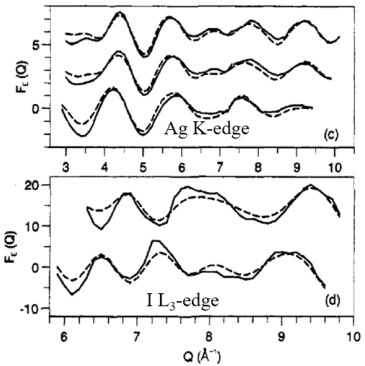

Experimental data (solid curves) and RMC fits (broken curves) for $(AgI)_x(AgPO_3)_{1-x}$ (top to bottom) x = 0.5, 0.3 and 0.0. EXAFS at (c) the Ag K-edge and (d) the I L_3-edge.

[1] S.J. Gurman and R.L. McGreevy, J. Phys.: Condens. Matter 2 (1990) 9463-9473.
[2] W. Bras, R. Xu, J.D. Wicks, F. van der Horst, M. Oversluizen, R.L. McGreevy, W. van der Lugt, Nucl. Instrum Meth. Phys. Res. A 346 (1994) 394-398.
[3] J.D. Wicks, L. Borjesson, G. Bushnell-Wye, W.S. Howells, R.L. McGreevy, Physica Scripta. T57 (1995) 127-132.

Reverse Monte Carlo Simulations of EXAFS Spectra (RMC-EXAFS)

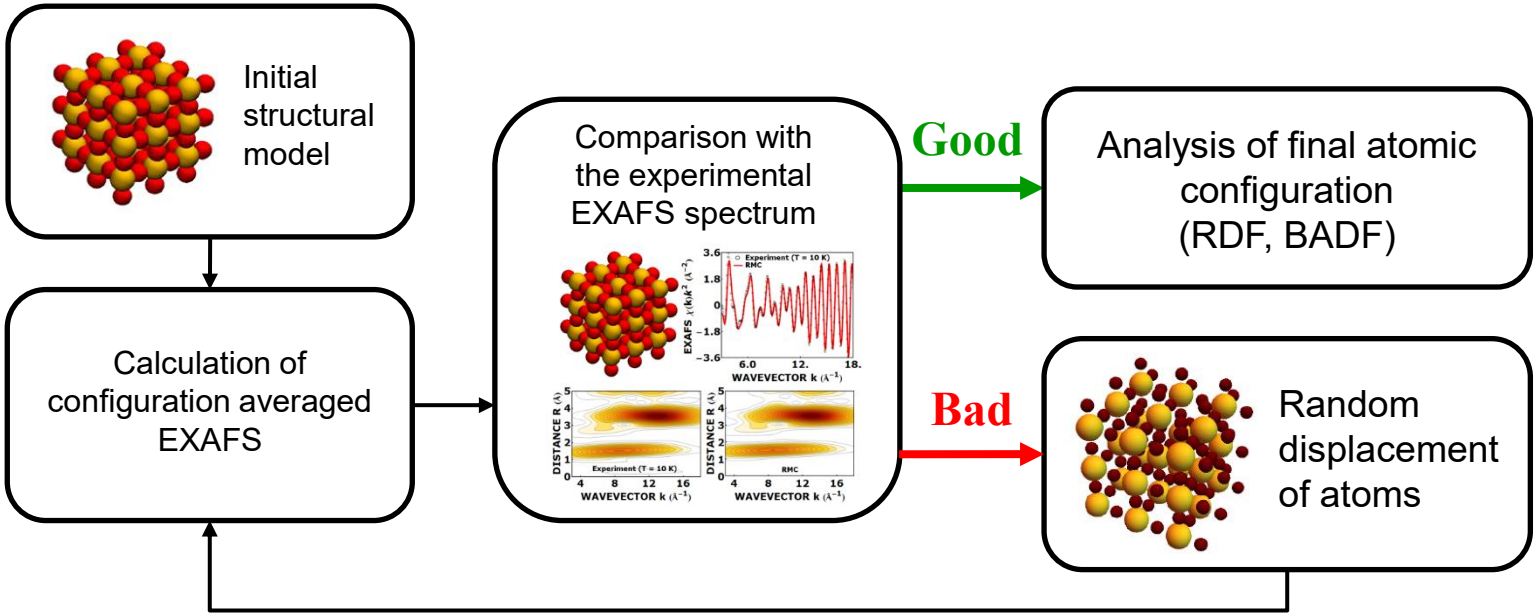

[1] R.L. McGreevy and L. Pusztai, Mol. Simul. 1 (1988) 359.
[2] J. Timoshenko, A. Kuzmin, J. Purans, J. Phys.: Condens. Matter 26 (2014) 055401.

Reverse Monte Carlo Method with Evolutionary Algorithm

EvAX code: Simulation-based analysis of EXAFS data for crystalline and nanocrystalline materials

(developed by Dr. Janis Timoshenko)

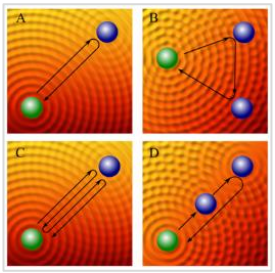

Multiple-scattering approximation

Reliable analysis of distant shells, partial RDFs and BADFs

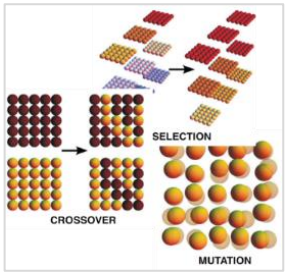

Evolutionary algorithm for optimization

Fast with good convergence

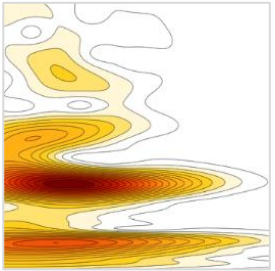

Wavelet transform for spectra comparison in *k* and *R* space

More reliable solution

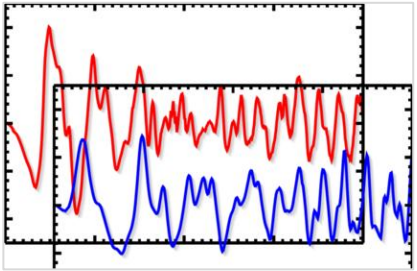

EXAFS spectra at several edges can be analysed simultaneously

One structural model

Code is available at https://www.dragon.lv/evax/

[1] J. Timoshenko, A. Kuzmin, J. Purans, J. Phys.: Condens. Matter 26 (2014) 055401.
[2] J. Timoshenko, A. Kuzmin, J. Purans, Comp. Phys. Commun. 183 (2012) 1237-1245.

Artificial Neural Networks (ANN) for X-ray Absorption Spectra Analysis

XANES

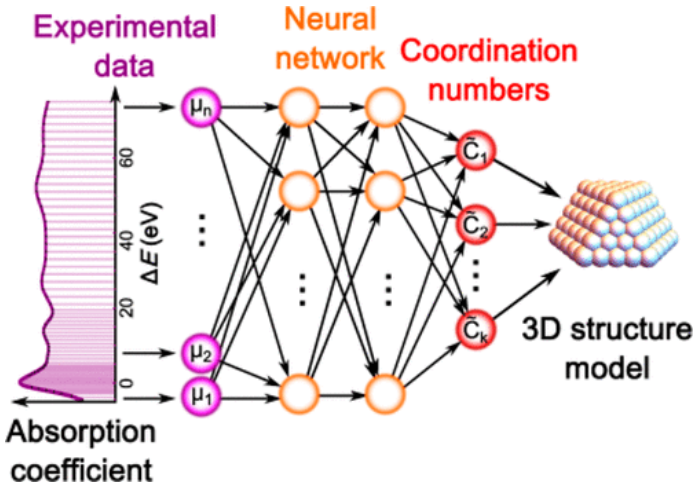

EXAFS

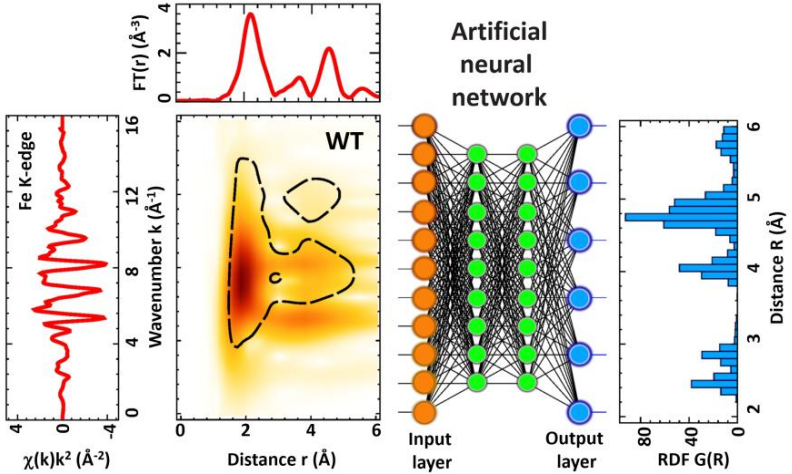

[1] J. Timoshenko, D. Lu, Y. Lin, A.I. Frenkel, J. Phys. Chem. Lett. 8 (2017) 5091-5098.

[2] J. Timoshenko, A. Anspoks, A. Cintins, A. Kuzmin, J. Purans, A.I. Frenkel, Phys. Rev. Lett. 120 (2018) 225502.

Examples of forward and inverse problem solving

Forward:

P. Žguns, I. Pudza, A. Kuzmin, Benchmarking CHGNet universal machine learning interatomic potential against DFT and EXAFS: Case of layered WS_2 and MoS_2, J. Chem. Theory Comput. 21 (2025) 8142–8150.

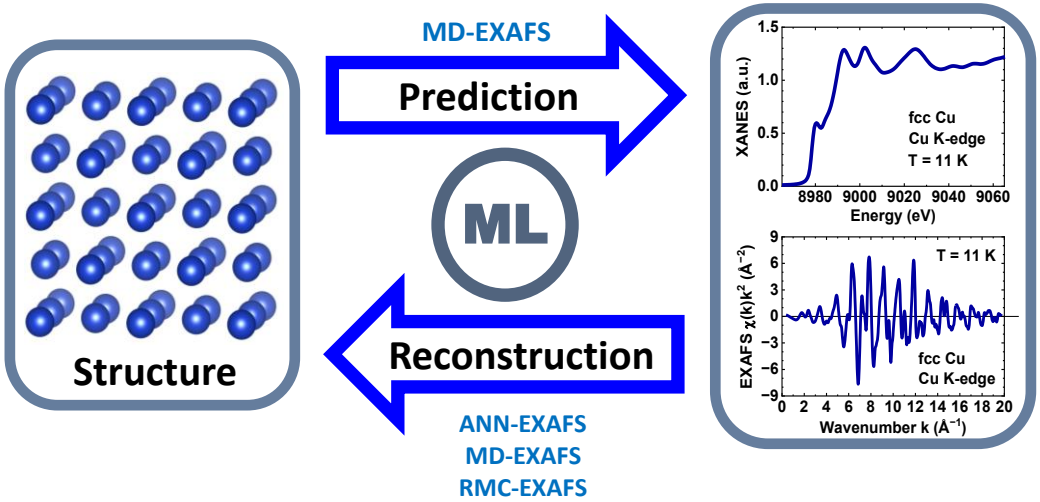

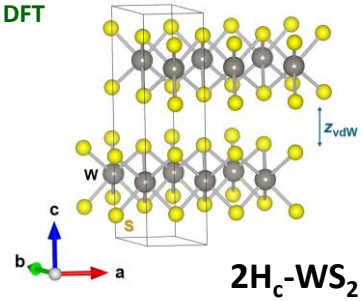

$2H_c$-WS_2

bcc α-Fe

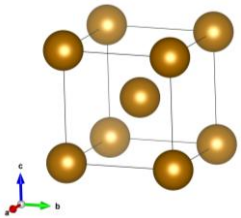

Inverse:

J. Timoshenko, A. Anspoks, A. Cintins, A. Kuzmin, J. Purans, A.I. Frenkel, Neural network approach for characterizing structural transformations by X-ray absorption fine structure spectroscopy, Phys. Rev. Lett. 120 (2018) 225502.

uMLIP CHGnet: Crystal Hamiltonian Graph Neural Network

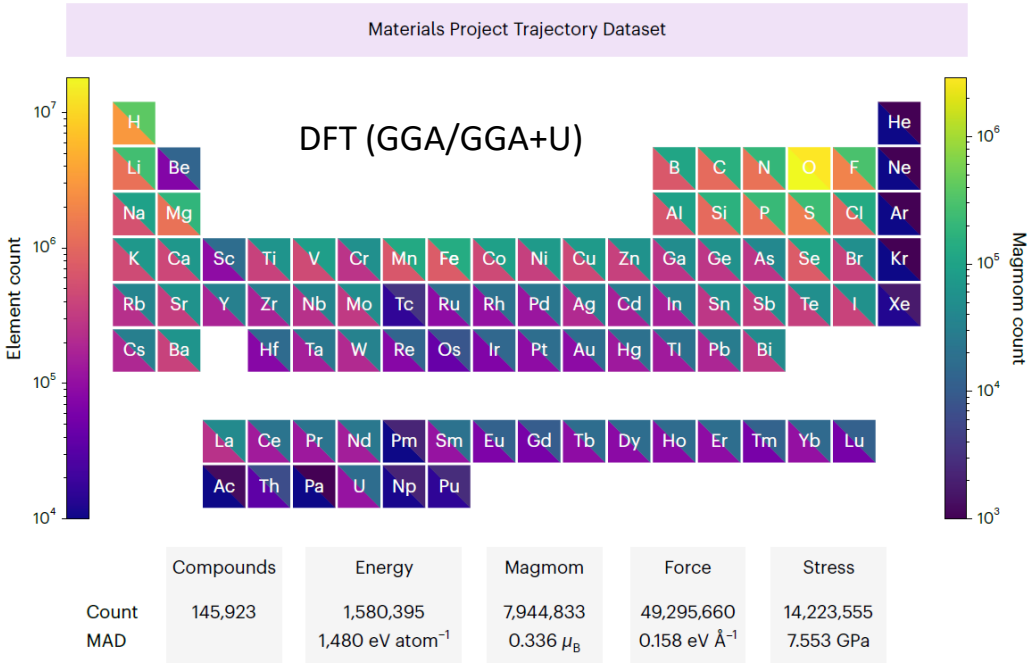

	Compounds	Energy	Magmom	Force	Stress
Count	145,923	1,580,395	7,944,833	49,295,660	14,223,555
MAD		1,480 eV atom^{-1}	0.336 μ_B	0.158 eV Å^{-1}	7.553 GPa

Universal Machine Learning Interatomic Potential (uMLIP)

Graph neural network **CHGNet** with 400438 trainable parameters was trained on the Materials Project Trajectory Dataset, split into training, validation, and test sets in a ratio of 8:1:1.

It can be fine-tuned!

The colour on the lower-left triangle indicates the total number of atoms/ions of an element.
The colour on the upper right indicates the number of times the atoms/ions are incorporated with magmom labels in the MPtrj dataset.
On the lower part of the plot is the count and mean absolute deviation (MAD) of energy, magmoms, force and stress.

B. Deng, P. Zhong, K. Jun, J. Riebesell, K. Han, C.J. Bartel, G. Ceder, Nat. Mach. Intell. 5 (2023) 1031–1041.

uMLIP: Vanilla & Tuned CHGNet vs DFT for layered WS_2

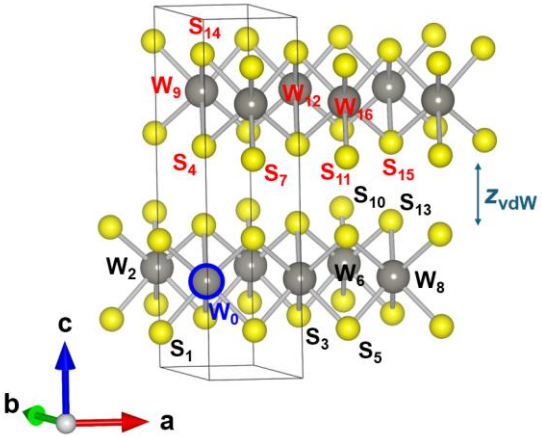

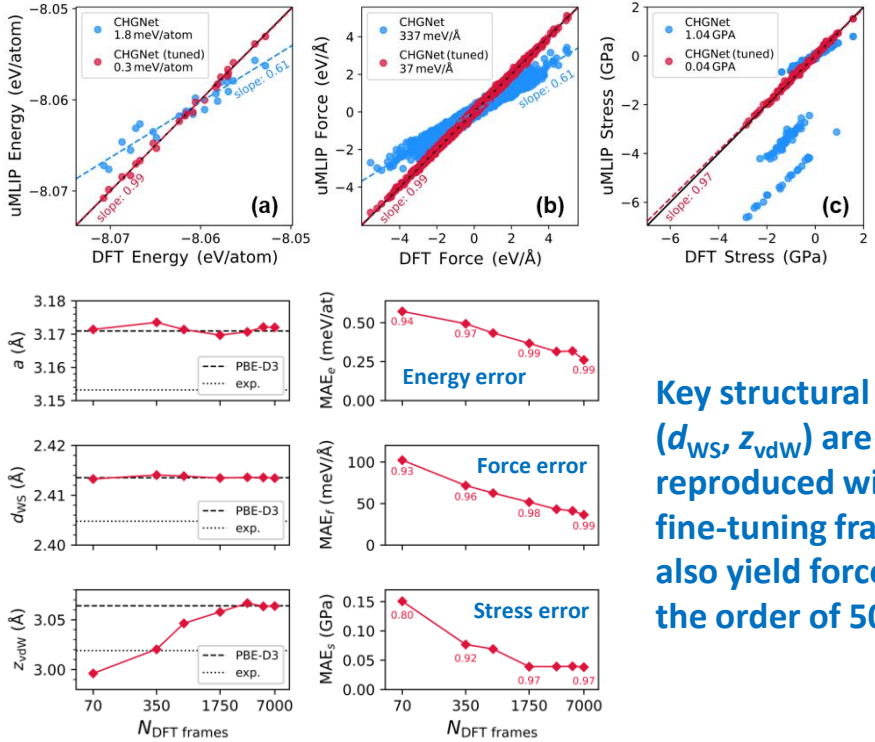

Key structural parameters (d_{WS}, z_{vdW}) are well reproduced with ~1000 fine-tuning frames, that also yield force accuracy on the order of 50 meV/Å.

P. Žguns, I. Pudza, A. Kuzmin, J. Chem. Theory Comput. 21 (2025) 8142–8150.

uMLIP: Vanilla vs Tuned CHGNet for layered WS_2

NVT MD
T=300 K

8a×8a×2c
supercell
(768 atoms)

Δt = 1 fs

Effect of tuning:

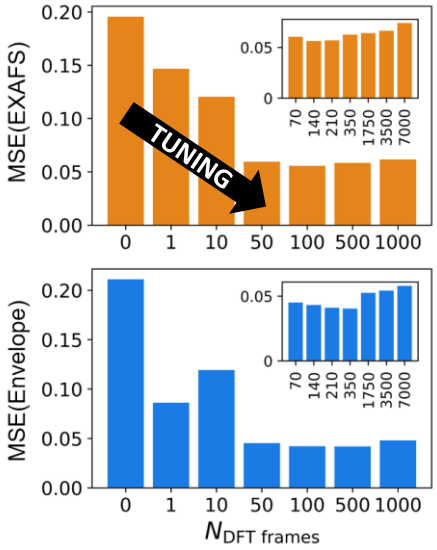

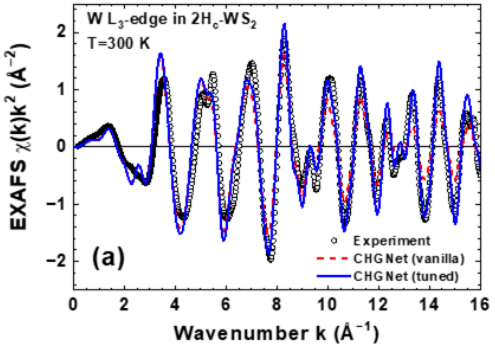

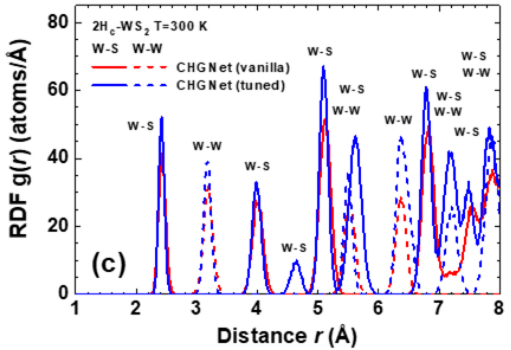

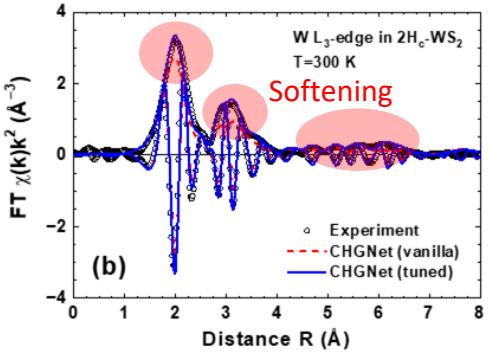

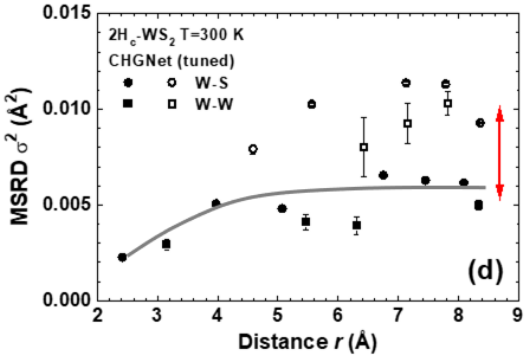

P. Žguns, I. Pudza, A. Kuzmin, J. Chem. Theory Comput. 21 (2025) 8142–8150.

uMLIP: Comparison with the best empirical potential

Empirical SWMBL-C potential was developed for bulk WS_2 and nanotubes in [1].

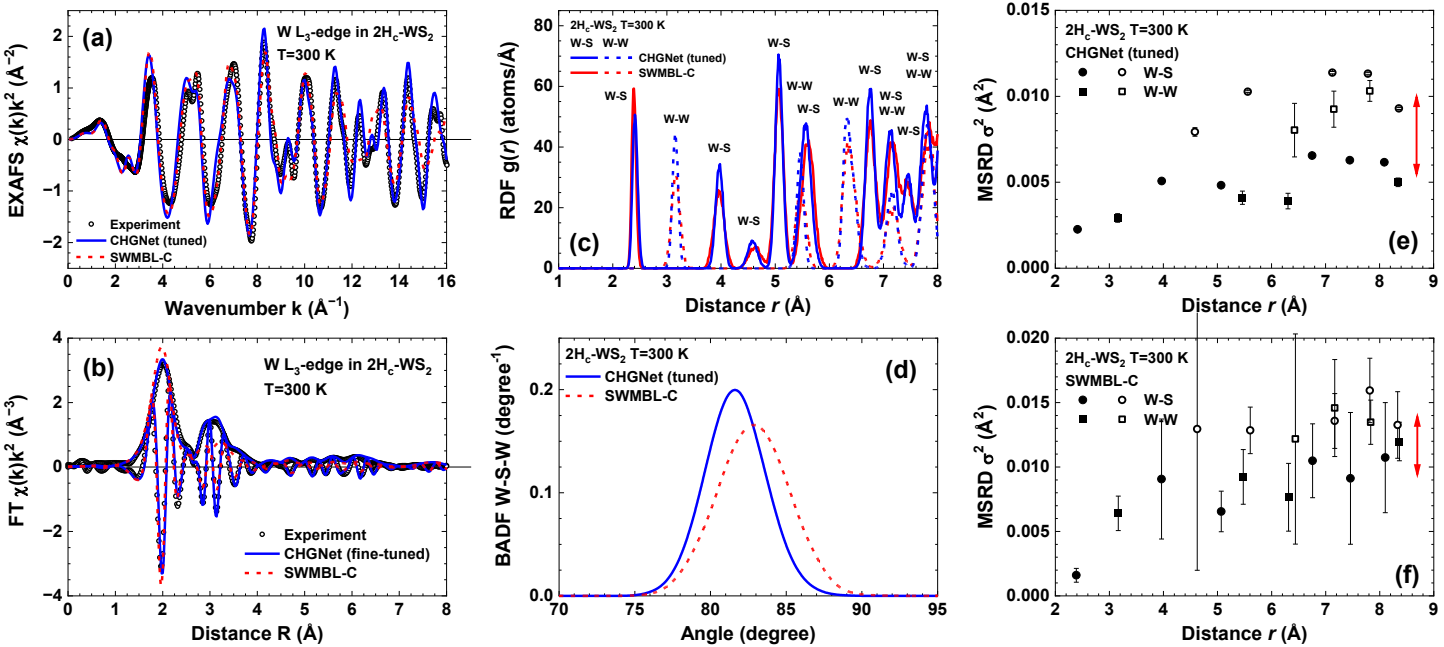

[1] A.V. Bandura, S.I. Lukyanov, A.V. Domnin, D.D. Kuruch, R.A. Evarestov, Comput. Theor. Chem. 1229 (2023) 114333.

Artificial Neural Network (ANN) Approach to EXAFS: Phase Transition in Iron (Fe)

In bulk Fe at temperature ca 1190 K (910 °C), the body-centered cubic structure (BCC) of α-phase (ferrite) changes to face-centered cubic structure (FCC) of γ-phase (austenite).

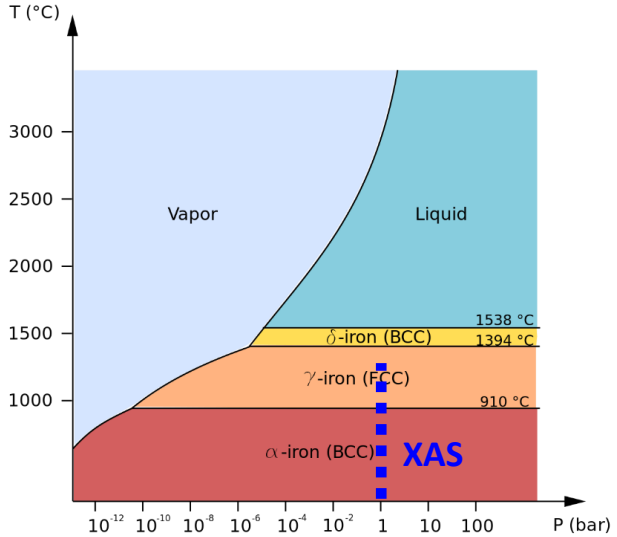

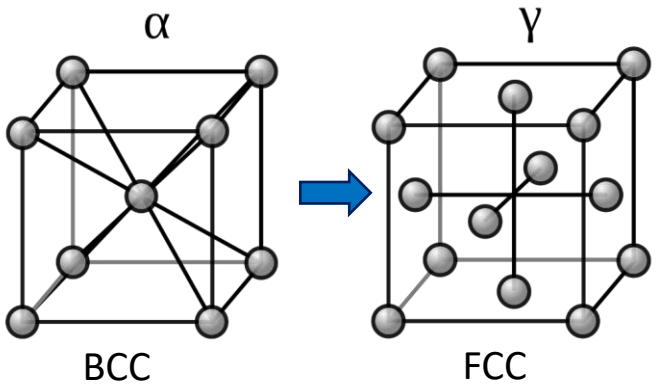

Z. Basinski, W. Hume-Rothery, A. Sutton, Proc. Royal Soc. London A 229 (1955) 459.

J. Timoshenko, A. Anspoks, A. Cintins, A. Kuzmin, J. Purans, A.I. Frenkel, Phys. Rev. Lett. 120 (2018) 225502.

Artificial Neural Network (ANN) Approach to EXAFS: Phase Transition in Iron (Fe)

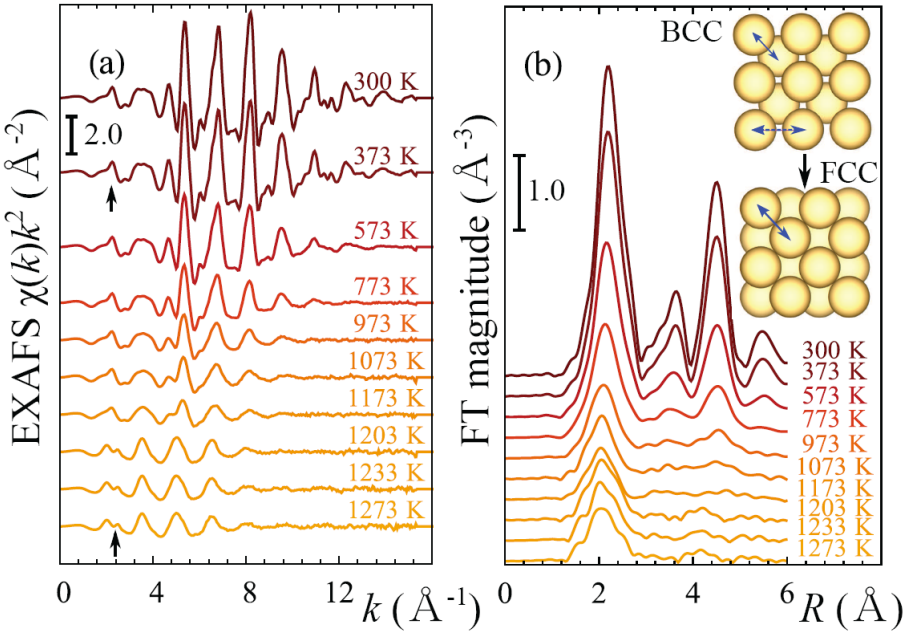

Experimental Fe K-edge EXAFS data of Fe

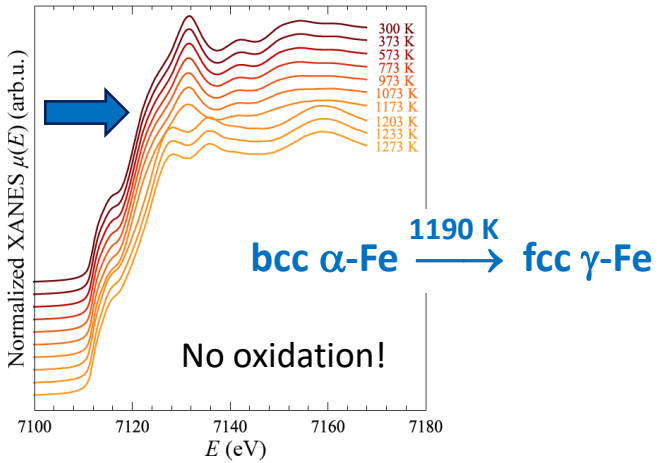

Sample: 4 µm Fe foil (99.99+% Goodfellow) packed between two BN pellets.

J. Timoshenko, A. Anspoks, A. Cintins, A. Kuzmin, J. Purans, A.I. Frenkel, Phys. Rev. Lett. 120 (2018) 225502.

Artificial Neural Network (ANN) Approach to EXAFS: Phase Transition in Iron (Fe)

Supervised learning based on MD

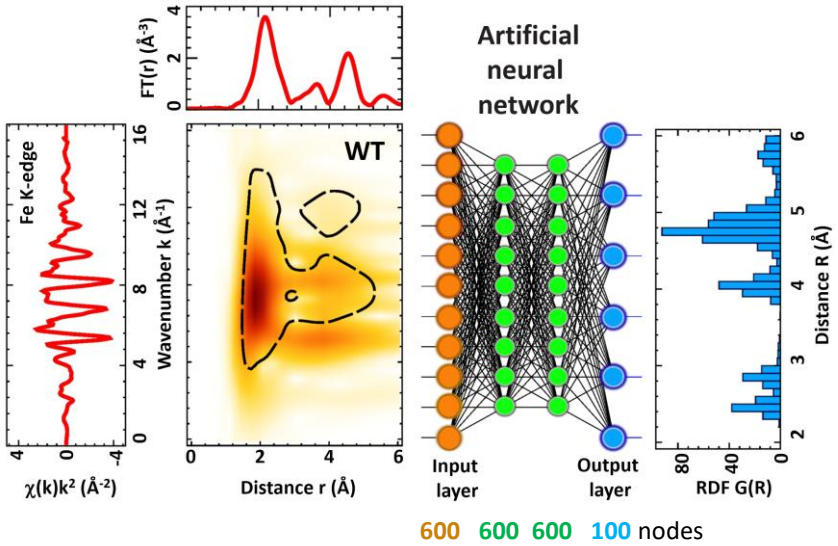

Classical NVT MD simulations were performed with GULP code (*J. D. Gale and A. L. Rohl, Mol. Simul. 29, 291 (2003)*) for iron with BCC, FCC and hexagonal close-packed (HCP) structures using Sutton-Chen type potential (modified Finnis–Sinclair (FS) potential) from *X. Dai et al., J. Phys: Condens. Matter 18, 4527 (2006)*.

We used 20 ps equilibration time plus 20 ps production time with the time step 0.5 fs. We used $5a_0x5a_0x5a_0$ supercell for BCC (250 atoms), $4a_0x4a_0x4a_0$ supercell for FCC (256 atoms) and $8a_0x4a_0x4c_0$ for HCP (256 atoms) phases. The lattice constant $a_0(T)$ was taken from XRD results for BCC and FCC Fe phases but of cobalt for HCP phase.

Temperature was varied in the range from 10 to 1500 K, and the lattice parameters were varied within 97%-103% to account for the thermal expansion of bulk iron.

3000 MD-EXAFS spectra were generated from MD configurations using FEFF8.5L code.

J. Timoshenko, A. Anspoks, A. Cintins, A. Kuzmin, J. Purans, A.I. Frenkel, Phys. Rev. Lett. 120 (2018) 225502.

Artificial Neural Network (ANN) Approach to EXAFS: Phase Transition in Iron (Fe)

Validation of the neural network with theoretical data (not used for NN training)

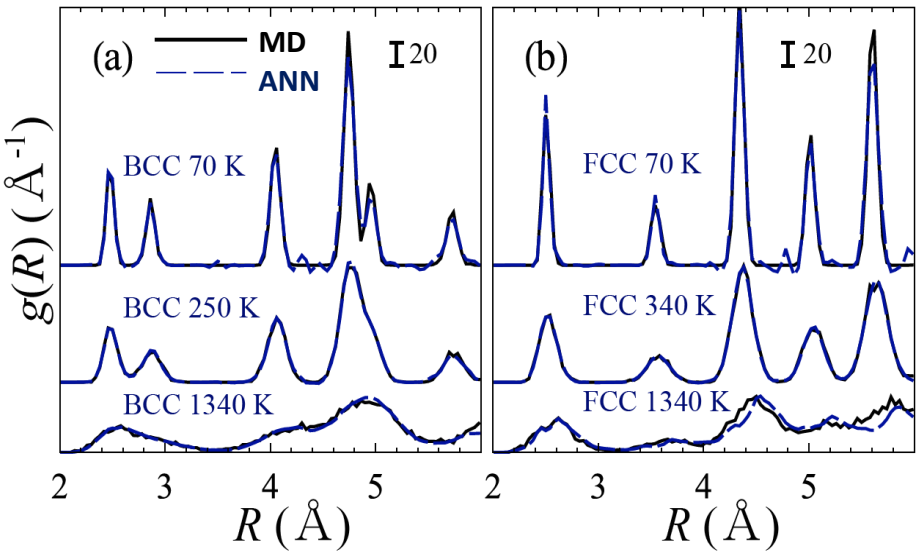

Reconstruction of RDF g(*R*) for bcc/fcc Fe, fcc Ni and hcp Co using neural network and RMC

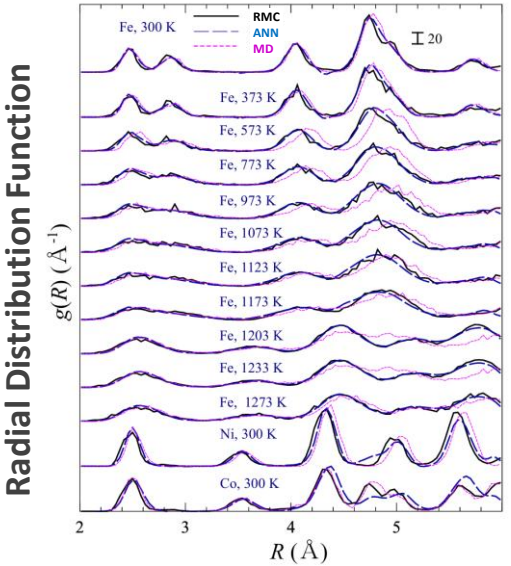

J. Timoshenko, A. Anspoks, A. Cintins, A. Kuzmin, J. Purans, A.I. Frenkel, Phys. Rev. Lett. 120 (2018) 225502.

Conclusions

- The use of Machine Learning (ML) methods in the **interpretation** and **prediction** of X-ray absorption spectra plays an important role in overcoming the limitations of traditional EXAFS/XANES analysis.

- Experimental EXAFS data, being sensitive to atomic structure and lattice dynamics, provide a valuable tool for **validating** the accuracy of MLIPs.

- ML methods are expected to enable the rapid and accurate processing of large experimental datasets, facilitate on-the-fly analysis and potentially automated experimental control.

https://www.dragon.lv/exafs/

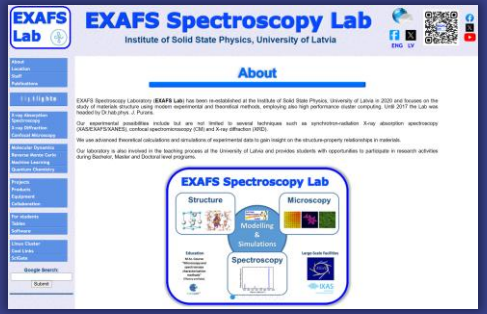

https://www.facebook.com/EXAFSLab/

Thank you for your attention!

LATVIJAS UNIVERSITĀTES
CIETVIELU FIZIKAS INSTITŪTS
INSTITUTE OF SOLID STATE PHYSICS
UNIVERSITY OF LATVIA

The work was supported by the Latvian Council of Science project No. LZP-2023/1-0476.

FLPP
FUNDAMENTAL AND APPLIED RESEARCH PROJECTS